



ELSEVIER

Deep-Sea Research II 52 (2005) 2018–2030

DEEP-SEA RESEARCH
PART II

www.elsevier.com/locate/dsr2

Weekly observations on dispersal and sink pathways of the terrigenous flux of the Ganga–Brahmaputra in the Bay of Bengal during NE monsoon

Onkar S. Chauhan^{a,*}, A.S. Rajawat^b, Yaswant Pradhan^b,
J. Suneethi^a, S.R. Nayak^b

^aNational Institute of Oceanography, Dona Paula, Goa 403004, India

^bSpace Application Centre, P.O., SAC, Ahmedabad 380015, India

Received 2 April 2003; accepted 23 May 2005

Abstract

The analyses of 64 sequential satellite images (October 1999–March 2001) of Indian Remote Sensing Satellite IRS—P4 ocean color monitor (OCM) (bands around 490, 555, and 670 nm) for total suspended matter (TSM), synchronous sea truth data acquisition, and salinity variations have been used to construct dispersal pathways of the surficial fluvial flux into the northern Bay of Bengal during the NE monsoon. From the spatial extent of the plumes of TSM (160–120 km) during October of 1999 and 2000, off the mouth of the Himalayan rivers the Ganga and the Brahmaputra (G–B), it is deduced that fluvial flux does not diminish concurrently with the termination of the southwest (SW) monsoon, as suggested by time-series trap experiments in the northern bay. During the NE monsoon, the G–B plumes move north to south initially off the mouth, and thereafter advects SW alongshore in the form of coastal sediment plumes, reducing the salinity of the coastal waters along the entire northern bay during October–December. We have observed a strong relation between enhanced episodic discharges of the Ganga–Brahmaputra (G–B) and augmented coastal turbidity during weekly events. It is also observed that even during such short (weekly) events of very high pulse of TSM discharge by the G–B system, the fluvial fluxes do not advect offshore into the deeper regions of the north-central bay, but are transported alongshore and distributed along the shelf. Our results, therefore, suggest that the reduced recovery of the fluxes in the sediments traps subsequent to the SW monsoon are not linearly related to the magnitude of fluvial flux of the G–B, but stems from the prevalent dispersal patterns.

© 2005 Elsevier Ltd. All rights reserved.

Keywords: Clays; Ocean color monitor; Dispersal pathways; Monsoon

*Corresponding author. Tel.: +91 832 2450338; fax: +91 832 2450603 05.

E-mail address: onkar@darya.nio.org (O.S. Chauhan).

1. Introduction

The Bay of Bengal is one of the largest fresh water and sediment input sites of the World Ocean (Emmel and Curray, 1984). The annual fresh water discharge into the bay exceeds $1.5 \times 10^{12} \text{ m}^3$, which reduces mean salinity by about 7‰ in its northernmost region (Laviolette, 1967). The bay receives about 2000 million tons of sediments annually contributed mainly by the Himalayan rivers—the Ganga and Brahmaputra; the Indian peninsular rivers—the Mahanadi, Godavari and Krishna; and Irrawadi and Salween from Myanmar.

Regulated by coupled differential heating and cooling of the Southern Indian Ocean and the Himalayas, there are two monsoons in the region. The southwest (SW) monsoon, prevalent during June–September, contributes about 80% of rainfall, which reduced considerably during the northeast (NE) monsoon (October–January). The varying intensities of the SW and the NE monsoons are interlinked, and it has been deduced that during the glaciation events in the Himalayas, when the land turned cooler, the NE monsoon was more intensely coupled with a weaker SW monsoon (Sarkar et al., 1990; Chauhan, 2003). The hydrography of the bay is also seasonal. Cyclonic (anticyclonic) equatorwards (polewards) currents are prevalent during NE (SW) monsoon (Shetye et al., 1991, 1993).

From time-series sediment trap experiments in the bay, it has been inferred that associated with peak discharge of the Himalayan rivers during the SW monsoon, terrigenous influx enhances many fold, and remains low for non-monsoon months (Ittekkot et al., 1991). Therefore, it was thought that the influx of terrigenous sediments into the bay is broadly regulated by precipitation or melting pulses from the Himalayas (Ittekkot et al., 1991). Moreover, a long-distance dispersal of these sediments by low salinity Bay of Bengal waters into the southeastern Arabian Sea and along the equatorial region, mostly during the NE monsoon has been documented (Shetye et al., 1991; Chauhan and Gujar, 1996).

The occurrence of high-magnitude, short-lived, cyclones/depressions in the bay are a common

phenomenon during the NE monsoon (Chauhan, 1995), and these bring torrential rains with sporadic fluvial discharge. Dispersal mechanism of the fluvial discharge into the bay is, therefore, complex, particularly during the NE monsoon. In the bay, time-series traps have been deployed to determine monthly fluxes at the selected locations (Ittekkot et al., 1991). These, being point observations, have limitations for estimating sediment flux of short weekly episodes during depression/cyclones or regional spatial variability of the TSM associated with localized episodic discharge from multiple fluvial sources in response to dynamic meteorological events. The sediment dispersal and sink pathways of fluvial suspended sediments, particularly during short (weekly) events, therefore remain in a state of infancy.

The Indian Remote Sensing Satellite (IRS—P4) was launched on May 26, 1999 by the Indian Space Research Organization. It has two oceanographic payloads, the Ocean Color Monitor (OCM) and the Microwave Scanning Multi-frequency Radiometer (MSMR). OCM is designed to measure the spectral variation of water leaving radiance that can be related to concentration of phytoplankton pigments, suspended sediment, colored dissolved organic matter (yellow substance or gelbstoff), and aerosols. OCM collects data in eight spectral channels (402–422, 433–453, 480–500, 500–520, 545–565, 660–680, 745–785, 845–885 nm) with a spatial resolution of 360 m, every alternate day for the same region at around 12 noon (local time) with radiometric resolution of 12 bits. The OCM scenes cover $1420 \text{ km} \times 1420 \text{ km}$ of ground area. In this paper, derived from the sequential analysis of IRS P-4 OCM and sea truth data, we present observations of short duration on the dispersal pathways of the suspended sediments discharged by the Ganga and the Brahmaputra Rivers during the NE monsoon.

2. Materials and methods

In order to obtain regional dispersal maps of the suspended sediments in the surficial waters for the NE monsoon season (October through January), among available imageries, 64 OCM images (path

Table 1
Details of the OCM imageries used in the present studies

| | Sensor | Cloud cover |
|------------------|--------|-------------|
| <i>Year 1999</i> | | |
| 11-Oct | OCM | Partial |
| 27-Oct-99 | OCM | Significant |
| 29-Oct-99 | OCM | Significant |
| 08-Nov | OCM | Partial |
| 10-Nov | OCM | Partial |
| 12-Nov | OCM | Partial |
| 14-Nov | OCM | Partial |
| 16-Nov | OCM | Partial |
| 02-Dec | OCM | Clear |
| 08-Dec | OCM | Partial |
| 12-Dec | OCM | Partial |
| 20-Dec | OCM | Partial |
| 24-Dec | OCM | Clear |
| <i>Year 2000</i> | | |
| 01-Jan | OCM | Partial |
| 07-Jan | OCM | Partial |
| 13-Jan | OCM | Partial |
| 17-Jan | OCM | Cloudy |
| 19-Jan | OCM | Partial |
| 23-Jan | OCM | Partial |
| 27-Jan | OCM | Partial |
| 06-Feb | OCM | Significant |
| 12-Feb | OCM | Clear |
| 18-Feb | OCM | Partial |
| 16-Feb | OCM | Significant |
| 28-Feb | OCM | Significant |
| 06-Mar | OCM | Significant |
| 18-Mar | OCM | Significant |
| 20-Mar | OCM | Partial |
| 26-Mar | OCM | Significant |
| 01-Oct | OCM | Significant |
| 05-Oct | OCM | Significant |
| 07-Oct | OCM | Partial |
| 17-Oct | OCM | Significant |
| 24-Oct | OCM | Partial |
| 30-Oct | OCM | Cloudy |
| 04-Nov | OCM | Partial |
| 08-Nov | OCM | Partial |
| 10-Nov | OCM | Significant |
| 18-Nov | OCM | Partial |
| 22-Nov | OCM | Clear |
| 28-Nov | OCM | Partial |
| 06-Dec | OCM | Cloudy |
| 08-Dec | OCM | Partial |
| 10-Dec | OCM | Clear |
| 18-Dec | OCM | Clear |
| 20-Dec | OCM | Clear |
| 22-Dec | OCM | Clear |
| 24-Dec | OCM | Clear |
| 28-Dec | OCM | Partial |
| 30-Dec | OCM | Clear |

Table 1 (continued)

| | Sensor | Cloud cover |
|------------------|--------|-------------|
| <i>Year 2001</i> | | |
| 01-Jan | OCM | Partial |
| 05-Jan | OCM | Significant |
| 09-Jan | OCM | Partial |
| 15-Jan | OCM | Clear |
| 17-Jan | OCM | Partial |
| 23-Jan | OCM | Partial |
| 27-Jan | OCM | Significant |
| 06-Feb | OCM | Partial |
| 10-Feb | OCM | Partial |
| 14-Feb | OCM | Partial |
| 18-Feb | OCM | Partial |
| 24-Feb | OCM | Partial |
| 28-Feb | OCM | Cloudy |

10, row 13, repeatability 2 days, zenith 1200 h) during October 1999–February 2001 were selected (generally 4–6 each month, Table 1) to determine the dispersal pattern of sediments in the study area. The OCM data were analyzed using the atmospheric correction and bio-optical algorithms developed initially for IRS-P3 MOS data (Mohan et al., 1998) and later modified for IRS-P4 OCM data (Chauhan et al., 2001).

For determination of dispersal patterns from OCM data, careful geometric correction and co-registration of the successive images within an error limit of one pixel is a prerequisite. A rotation between the images reduces the matching coherency and a translation shift reduces the matching accuracy. A two-stage approach was followed for geometric corrections. First, a geometric correction was applied separately on the individual data set to remove image distortion and bring them to a standard geographic projection, with Modified Everest datum (i.e. a local geodetic datum, based on Everest spheroid that best fits to extent of the Indian subcontinent). In the second stage, co-registration was done by warping one image to the other using polynomial transformation. The transformation was defined by matching more than 25 pairs (as many as possible) of Ground Control Points (GCP) on the images, selected from identifiable coastline features surrounding the study area. The re-sampling at both the stages

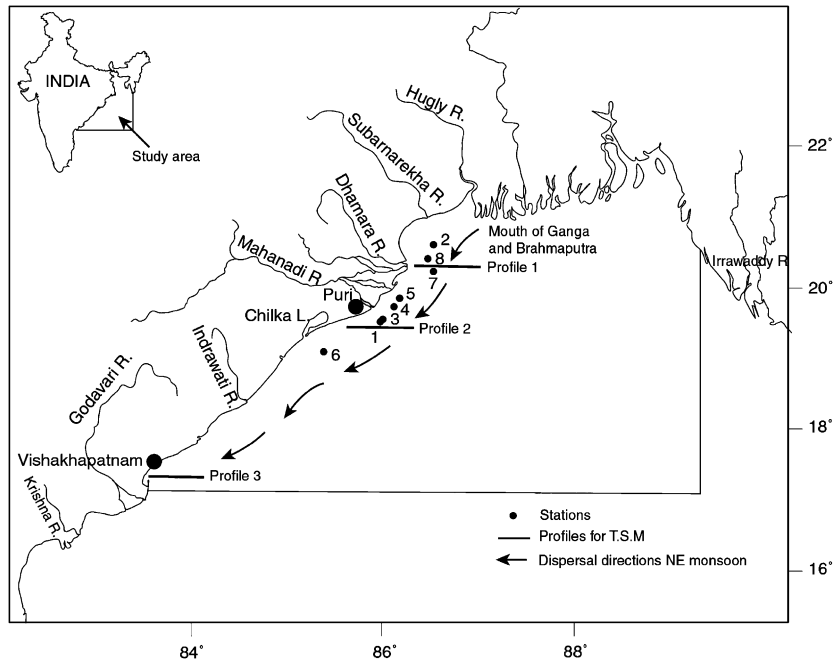


Fig. 1. The study area and locations of the sampling stations for clays analysis. The profiles taken for temporal and spatial variations along the East Coast of India also are shown.

was performed by cubic convolution interpolation techniques to keep the spatial distortions at a minimum (Legeckis and Pitchard, 1976; Emery and Ikeda, 1984). The images could be co-registered within an error limit of one pixel (~ 360 m).

The suspended sediment concentrations in the coastal areas have been derived using water-leaving radiance in band 490, 555 and 670 nm. The modified algorithm of Tassan (1994) has been used to compute suspended sediment concentrations from OCM from the following relation:

$$\text{Log } S = 1.83 + 1.26 \text{ Log } X_s$$

$$\text{for } 0.0 \leq S \leq 100.0,$$

where S is suspended sediment concentration in mg/l and X_s is variable defined as

$$X_s = [\text{Rrs}(555) + \text{Rrs}(670)] \\ \times [\text{Rrs}(490)/\text{Rrs}(555)]^{-0.5}.$$

$\text{Rrs}(\lambda)$ is remote sensing reflectance in respective wavelengths.

In situ, pass-synchronous measurements of suspended sediments (retained on $<0.2 \mu\text{m}$ optipure fiber filter paper) and currents at 52 stations were carried out on board R.V. *Samudra Kaustubh* and locally acquired fishing crafts. The currents were measured by CONTROL Ocean current meter (accuracy of $\pm 5^\circ$ and 2% for direction and magnitude, respectively). The global positioning system (GPS) was used for determining the geographical location of each point.

In the surface seawaters of the bay, for determining clay abundance, terrigenous matter was separated through six feet, Prep/Scale TFF regenerated cellulose cartridge (No. CDUF 006 Lm) and a tangential flow filtration system of Millipore, which separates $\sim 0.02 \mu\text{m}$ size particulate matter from sea water. About 100–150 l of seawater were filtered for each station for acquiring about 200–300 mg of TSM during November of 2000 at eight stations along Orissa Coast (Fig. 1). Owing to a very small amount of sample for clay mineral analysis, a fraction of these samples was passed through a membrane filter of

Table 2

In situ current vectors and advective velocity vectors derived by maximum cross correlation pattern matching method applied on sequential IRS-P4 OCM data of the northern Bay of Bengal (see Prasad et al., 2002, for methodology)

| Sr. no. | Latitude (North) | Longitude (East) | In situ magnitude (cm/s) | Derived magnitude (cm/s) | In situ direction (deg) | Derived direction (deg) |
|---------|------------------|------------------|--------------------------|--------------------------|-------------------------|-------------------------|
| 1 | 19.05 | 85.47 | 6 | 9.5 | 195 | 210 |
| 2 | 20.97 | 87.16 | 12 | 10.0 | 312 | 288 |
| 3 | 20.02 | 87.21 | 10 | 12.0 | 71 | 84 |
| 4 | 21.07 | 87.16 | 15 | 13.5 | 185 | 172 |
| 5 | 20.83 | 87.21 | 15 | 13.6 | 60 | 65 |
| 6 | 20.97 | 87.26 | 16 | 15.9 | 73 | 75 |
| 7 | 21.07 | 87.26 | 16 | 17.5 | 217 | 216 |
| 8 | 20.91 | 87.26 | 20 | 18.6 | 253 | 278 |
| 9 | 20.97 | 87.31 | 23 | 21.9 | 45 | 45 |
| 10 | 20.71 | 87.31 | 26 | 23.9 | 255 | 280 |
| 11 | 20.91 | 87.31 | 22 | 23.9 | 330 | 338 |
| 12 | 21.08 | 87.21 | 24 | 25.0 | 193 | 188 |
| 13 | 20.96 | 87.21 | 28 | 28.2 | 50 | 47 |
| 14 | 19.12 | 85.60 | 35 | 29.4 | 260 | 270 |
| 15 | 20.66 | 87.28 | 29 | 32.6 | 200 | 205 |
| 16 | 20.97 | 87.36 | 41 | 39.8 | 216 | 208 |
| 17 | 20.02 | 87.36 | 46 | 48 | 178 | 181 |

$\sim 2\mu\text{m}$. The collected clays on filter paper were dispersed on a glass slide to obtain an oriented sample. The glycolated (treated for 2 h with ethyleneglycol at 100°C) samples were analyzed on X-ray diffractometer (Phillips 1840) for identification. Clays were identified and quantified using the methods of Biscaye (1965).

By and large, the correlation between the sea truth and imageries data of TSM is moderate ($r = 0.51$, $p = 0.001$; Anuradha et al., 2000). Because of the complexities and inherent limitation of available algorithms, TSM concentrations derived from the image are underestimated compared to in situ measurements (Anuradha et al., 2000). However, imagery-derived dispersal parameters in our other study have high correlations with measured in situ current magnitudes and directions (Prasad et al., 2002; Table 2; Fig. 4). Although TSM patterns derived from the imageries in the study area have limitation for the accurate quantification of fluxes, they can be used in conjunction with measured TSM and current parameters for the reconstruction of regional dispersal patterns of the fluvial flux. The sequential variations in TSM on digitally enlarged scenes of

IRS-P4 OCM data were studied to determine regional dispersal patterns and sink pathways of the sediments discharged by the G–B system, supplemented by the measured in situ current, sea-surface salinity (SSS) variations, and characteristic clays in the surface waters. The spatial and temporal variations of TSM along 160–200 km selected W–E transects (Fig. 1) also were evaluated during events of short-duration fluvial pulses of high TSM.

3. Results and discussion

The generalized TSM patterns have large spatial and temporal variations during the NE monsoon. During the month of October, 120–160 km-wide plume of the G–B system has been traced (Fig. 2A). During the months of November, however, there are frequent, short-duration pulses of high TSM (Figs. 2C–D). Gradually, the influx of TSM is reduced during December–January (Fig. 3). The measured and imagery-derived current vectors for the study area are presented in Fig. 4. Based upon these results, it is deduced

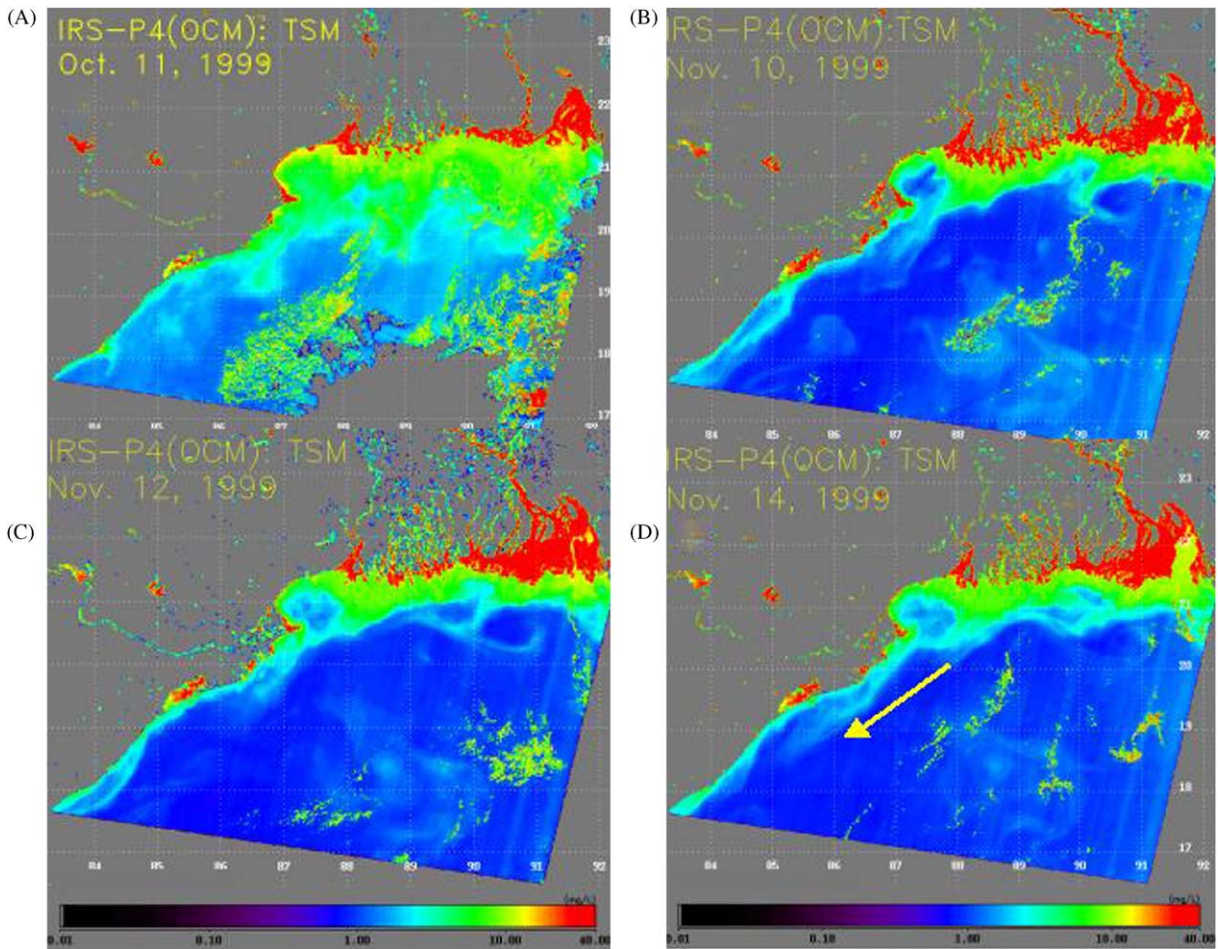


Fig. 2. TSM maps for October–November 1999. Scenes (B–D) show weekly pulses of high TSM from the Himalayan source and their alongshore advection. Arrow indicates the dispersal direction of the sediments.

that the currents, by and large, are equatorwards. The temporal monthly variations in TSM along three W–E Profiles (Fig. 1) are presented in Fig. 5.

3.1. TSM patterns from the satellite imageries

During the October of 1999–2000, we have mapped offshore extension of the plume of the G–B system to be 120–160 km. These results imply that concurrent with the cessation of the SW monsoon, the influx of fluvial flux does not dwindle as observed in the time-series traps (Ittekkot et al., 1991). The dispersal pattern

derived from the sequential scenes and from the insitu TSM measurements is south–SW (Fig. 2A). In situ pass synchronously measured current directions are equatorward irrespective of the tidal phase, except off the mouth of the G–B system where the circulation and dispersal are influenced by the prevalent macrotidal regime, and the observed currents are N–S (Fig. 4). Evaluated separately, the imagery-derived magnitudes and directions of surficial currents and dispersal directions of TSM are significantly correlated with measured sea-truth observations ($r = 0.99$, $p = 0.001$; Prasad et al., 2002; Table 2; Fig. 4).

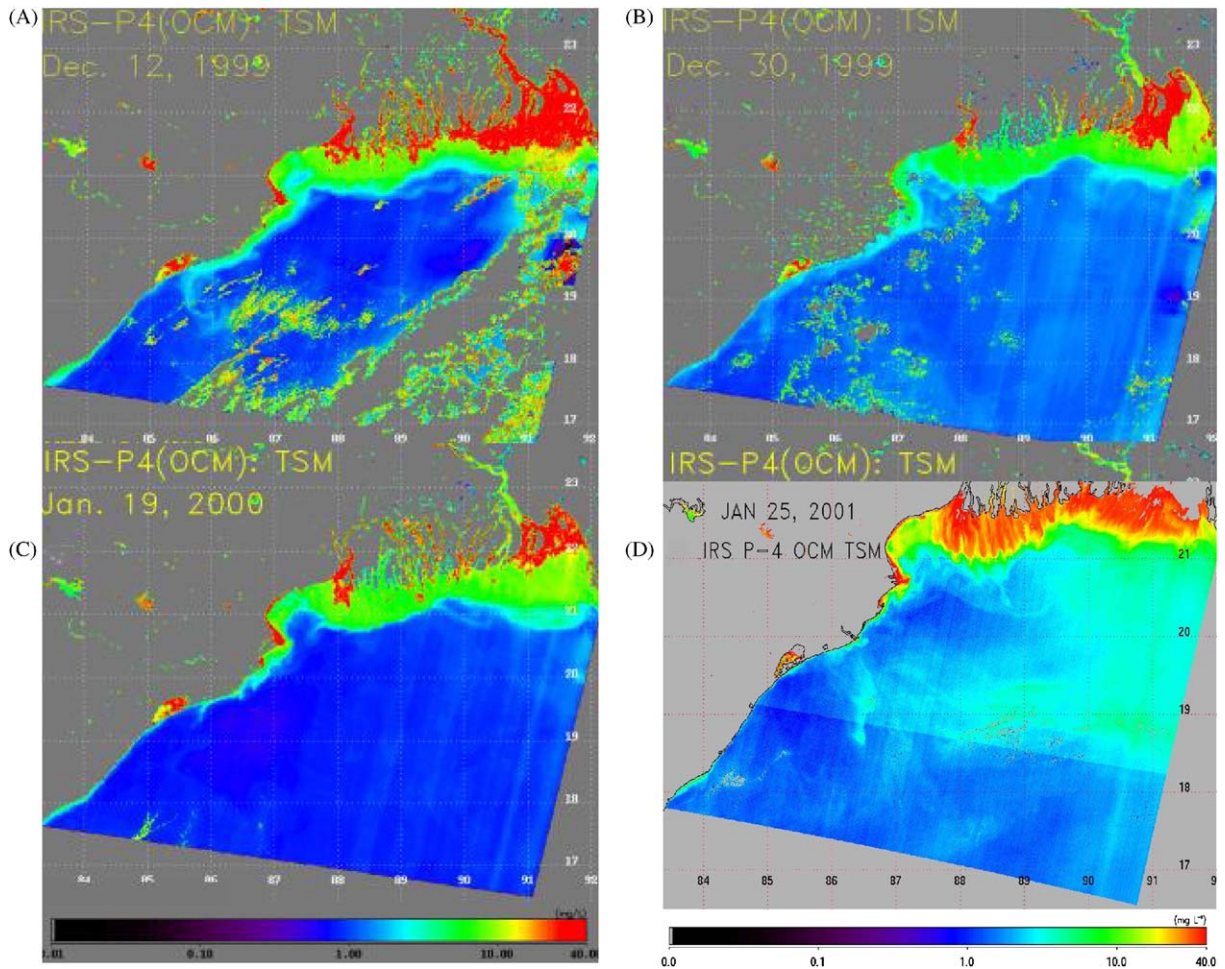


Fig. 3. Generalized maps of TSM during December 1999 and January 2000–2001. Cross-shelf dispersal off the TSM off the Chilika Lake (scene A) is a distinct, short-duration dynamic feature.

The circulation in the area during October is mostly equatorwards and sets in early October.

During November of 1999–2000, the generalized pattern of the suspended sediments is similar to the one observed in October (Figs. 2B–D, 4). The aerial extent of the plume, off the mouth of the G–B, also remains unchanged during different tidal phases in November. However, there is a high temporal variability in the fluvial plume characteristics with frequent, short-duration, high-TSM pulses from the G–B. To elucidate the dispersal

of sediments during such events, a weekly event observed during 8–14 November 1999 has been evaluated. On the imagery of 8 November 1999, there was a sporadic increase in the spatial extent as well as TSM contents of the G–B plume. In the subsequent imagery of 10, 12 and 14 November 1999, this pulse is observed to have dispersed in narrow bands all along inner shelf region (Figs. 2C and D). The sequential variations in the TSM along the three W–E profiles in the northern, central, and southern regions (Fig. 1) between 8 and 14 November 1999 (Figs. 6–8) also are

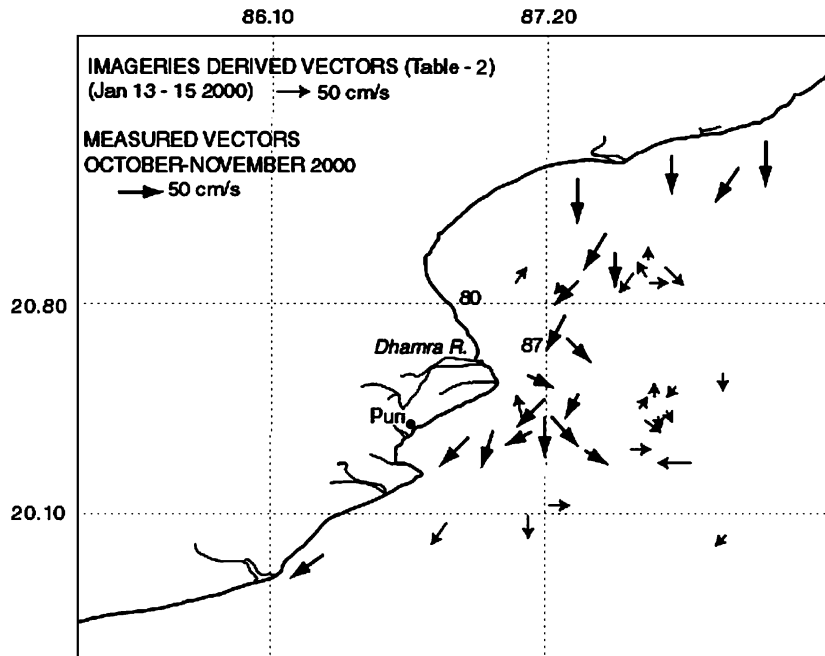


Fig. 4. The measured velocity vectors during October–November of 2000 (thick arrows). Vectors derived from imageries (thin arrows), details of which is given in Table 2, also are shown.

evaluated to further elaborate the pathways of TSM dispersal. On all individual profiles, from the north (off the Dhamra River) to the southern region (off Visakhapatnam), in the inland waters, there was a distinct localized area of high TSM, which decreased offshore on all the profiles, except on Profile 1 where a high TSM band existed at about 100 km offshore. On the subsequent profiles of 10 November 1999, in addition to the inland TSM enrichment, an additional band of high TSM, located about 50–100 km offshore also was observed. Between these two TSM-enriched water masses, reduced TSM values were found. These two water masses, therefore, have different sources of TSM—the offshore one from the pluses of the G–B system. There was a sequential change in the location of the plume (spread between 50 and 100 km offshore on 12 November; 30–50 km on 14 November; Figs. 2C and D, 6–8), which implies an inland migration of this plume. We infer that the fluvial discharge of the Himalayan rivers advects alongshore in narrow localized bands. The time

span for the advection of TSM plume from Profile 1 to 3 had been 6 days, which implies that dispersal rate is rather rapid (over 250 km in 6 days). These results distinctly suggest that the equatorwards hydrography is highly dynamic and disperses the fluvial influx along the shelf in short span of time.

3.2. Clay minerals

In order to further elucidate source of the fluxes, the clay minerals transported in the seawaters during November of 2000 have been evaluated. The clays can be used as tracers as they have the following: (i) mean grain size $< 2 \mu\text{m}$, (ii) a potential to be transported regionally in suspension, (iii) regulation by geology and drainage characteristics of catchment area, and (iv) fluvial source specific assemblage. The clays present in the surface waters along the study area are illite, chlorite, kaolinite, and smectite (traces) in the order of abundance in the northern bay (Table 3). This clay mineral assemblage is a characteristic of

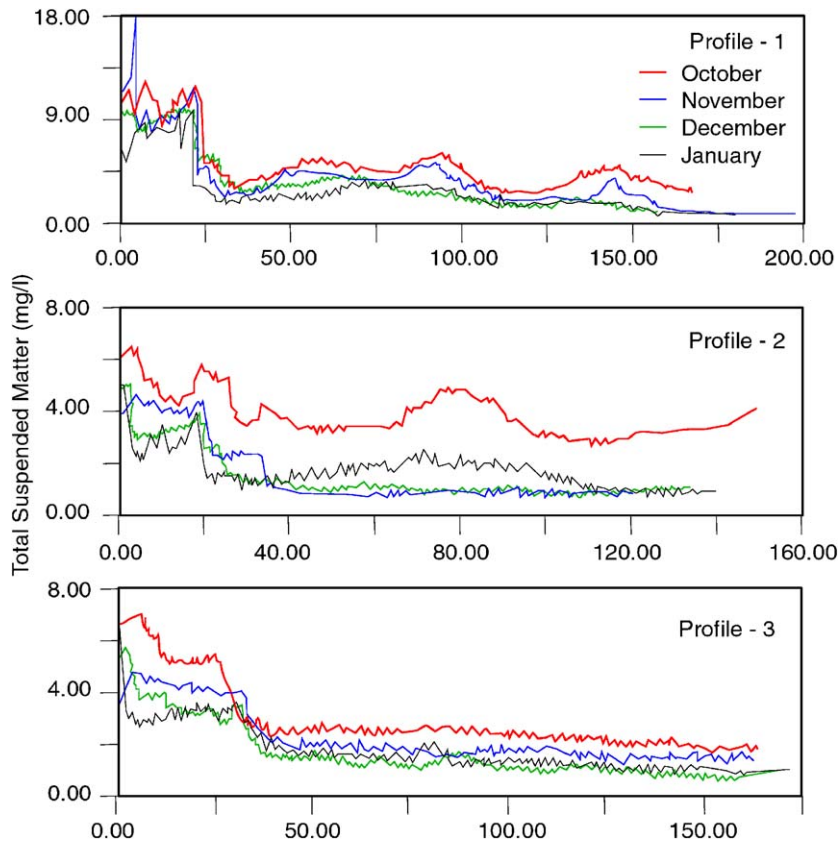


Fig. 5. Monthly variations in TSM along Profiles 1–3 in the northern Bay of Bengal.

the load of the G–B system (Konta, 1985), suggesting that fluvial flux of the G–B system is dispersed and distributed along the shelf by the equatorward hydrography.

Chlorite, a clay produced under arid, cold climate is reported by Rao et al. (1988), along the continental shelf off Orissa. It is however not contributed from the Mahanadi, in contrast to what has been suggested by Rao et al. (1988), because O.S. Chauhan, Y. Pradhan and J. Suneethi (unpublished data) has found smectite, illite, kaolinite in the river load of the distributaries of the River Mahanadi related with geology and humid tropical climate prevalent in the catchment area. The integrated results of the present study, for the first time, distinctly suggest higher influence of the G–B system onto the coastal regions off the

northern Bay of Bengal. The reduced terrigenous flux into the central and the northern traps of the Bay of Bengal during the NE monsoon therefore appear to be linked with the dispersal mechanism, rather than being linearly related to the magnitude of the flux from the G–B. These observations have implications for the biogenic processes and sink of the carbon related to sediment dispersal during the Heinrich events when the NE monsoon was stronger.

3.3. Sea-surface salinities

The seasonal SSS maps of the northern Indian Ocean derived from available in situ observations (Levitus et al. (1994), and available data with data center of the National Institute of Oceanography,

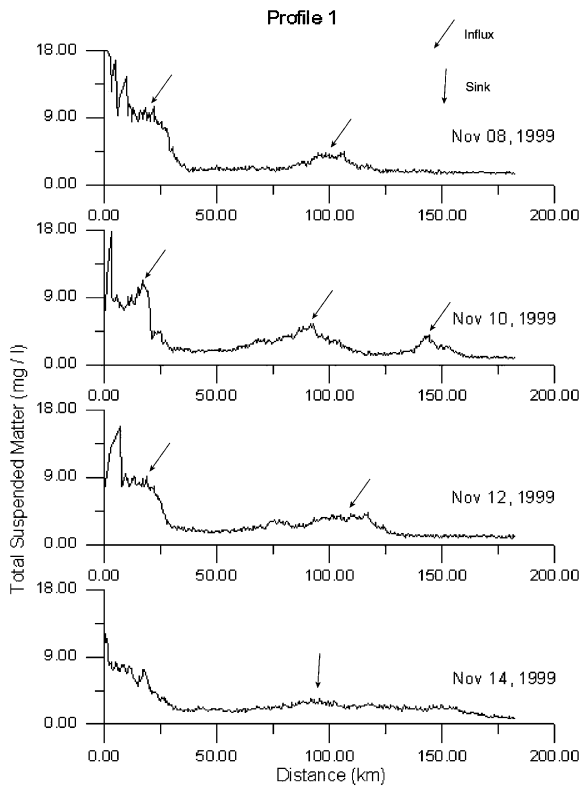


Fig. 6. Weekly, spatial and temporal variations in the TSM along W–E Profile 1, off the mouth of Mahanadi–Dhamra. Note the inland shift of plume in coastal waters during 8–14 November 1999. Arrows indicate influx and sinking of the TSM.

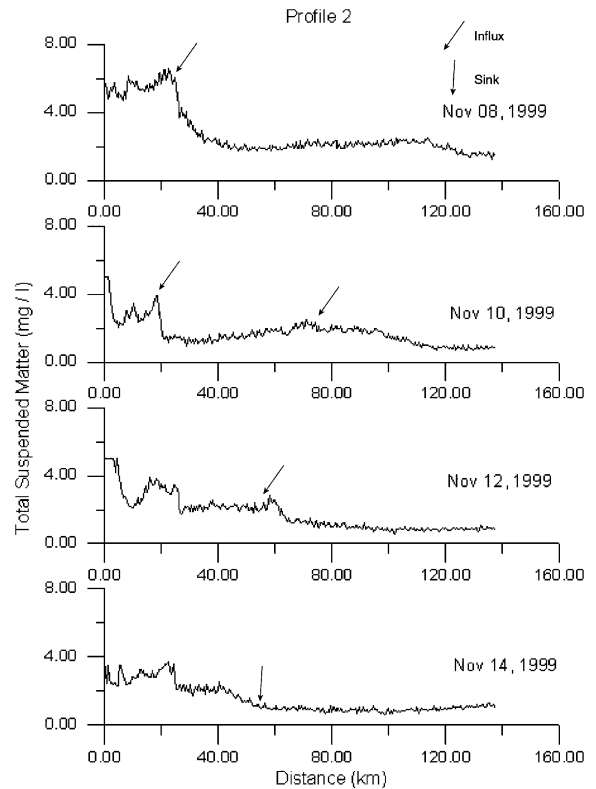


Fig. 7. Same as Fig. 6, but of W–E profile south off Paradeep (Profile 2). Sequential increase of TSM from offshore into inland waters and a time lag of 2 days with respect of Profile 1, is a distinct feature.

Goa) are also evaluated in order to examine the advection of the fluvial flux during the SW and the NE monsoon (Fig. 9). The SSS during the SW monsoon are low, as expected, with wide offshore extension of low salinities down to 15°N latitude. During October–December, along the entire northern coast of the Bay of Bengal, the SSS is also reduced (Fig. 9). The freshwater flux by northern coastal rivers the Dhamara and the Mahanadi into the bay after cessation of the SW monsoon is reduced many fold. The local fluvial discharge is, therefore, not sufficient to sustain lower regional salinity all along the coastal waters. A seasonal low in SSS all along the shelf of the study area therefore appears to stem from the equatorward advection and

dispersal of the fluvial fresh water plume of the G–B.

3.4. Interannual TSM variations

There is no significant change in the regional direction of the suspended sediment dispersal in December 1999–2000 and January 2000–2001, which by and large remains southerly to south-westerly (Fig. 3). However, compared to November 1999 the turbid plume off the Sand Head flows farther inshore (area extent about 30–40 km) during December 1999–2000 and January 2000–2001. There are also some sporadic short-term (weekly) changes in the dispersal patterns; most prominent among them is observed off

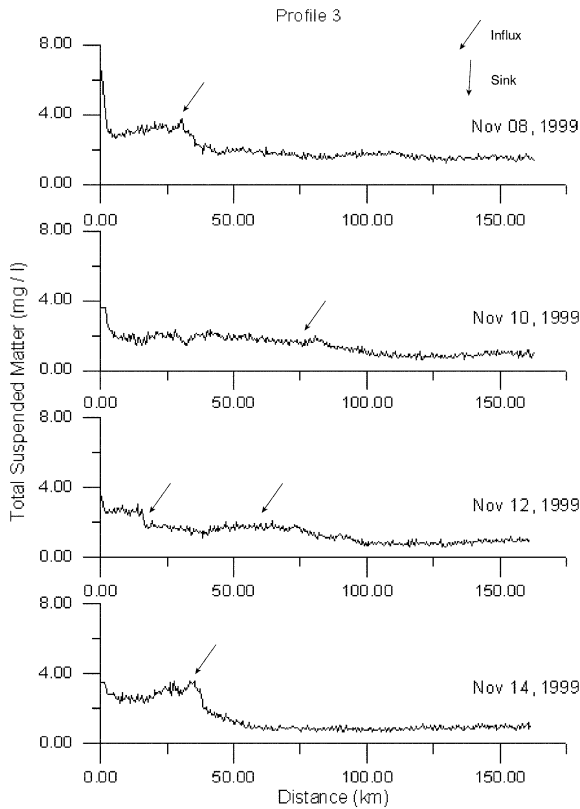


Fig. 8. Same as Fig. 6, but for Profile 3 off Visakhapatnam. Sequential delay in the enrichment of TSM in coastal waters after a time lag (initiated on 10 and prominent on 12 November, 1999) related with the enhanced influx from the Himalayan Rivers is observed.

Chilika lagoon. Disrupting the southwesterly alongshore dispersal of the sediments of the Ganga–Brahmaputra source, for a brief period, across shelf dispersal of sediments (spatial extension about 50 km) into the deeper offshore region has been archived (Fig. 3A). Derived from the average monthly mean for the years 1999–2000, the time series variations in the TSM at Profiles 1–3 distinctly show different trends for coastal and offshore waters during October through January (Fig. 5). At all the profiles, the coastal waters have higher TSM. However, being in the vicinity of the G–B, the area off the Dhamara River continues to have much wider spatial extent

Table 3

Clay abundance (weighted percent) in the suspended sediments (water depth 0–2 m) at selected locations. Refer to Fig. 1 for location of the stations

| Station no. | Location | Water depth (m) | Illite | K + C | K/C | Smectite |
|-------------|--------------------------|-----------------|--------|-------|------|----------|
| 1 | 19°40.10N 85°50.13E | 22 | 61 | 17.9 | 1.58 | 5.1 |
| 2 | 21°05.544N 87°09.87E | 20.4 | 67 | 17.3 | 1.48 | 5.6 |
| 3 | 19°40.15N 85°50.21E | 32 | 61 | 16.9 | 1.51 | 5.4 |
| 4 | 20°04.03N 86°50.01E | 52.5 | 70.9 | 19.8 | 0.56 | 5.8 |
| 5 | 19°55.146N 86°28.47E | 32 | 73.1 | 15.5 | 0.61 | 6.4 |
| 6 | 19°03.386N 85°28.659E | 295 | 61.4 | 17.9 | 0.78 | 6.5 |
| 7 | 20°42.614N 87°19.14 E | 28 | 69.4 | 19.8 | 0.63 | 5.1 |
| 8 | 20°50.011N 87°12.92 E | 24.2 | 67.2 | 17.8 | 0.68 | 5.8 |

and higher TSM during the entire season of the NE monsoon. In the offshore waters, however, the TSM is much reduced, except in a few isolated areas.

4. Conclusions

From these observations, we deduced the following:

- (1) During the NE monsoon the suspended sediment influx of the G–B system influences the coastal processes with much higher spatial variability along the northern region than previously envisioned.
- (2) The supply of the terrigenous sediments to the deeper off shore regions of the central bay during the NE monsoon is not related with the magnitude of influx of the sediments into the bay, but the prevalent dispersal by the hydrography.

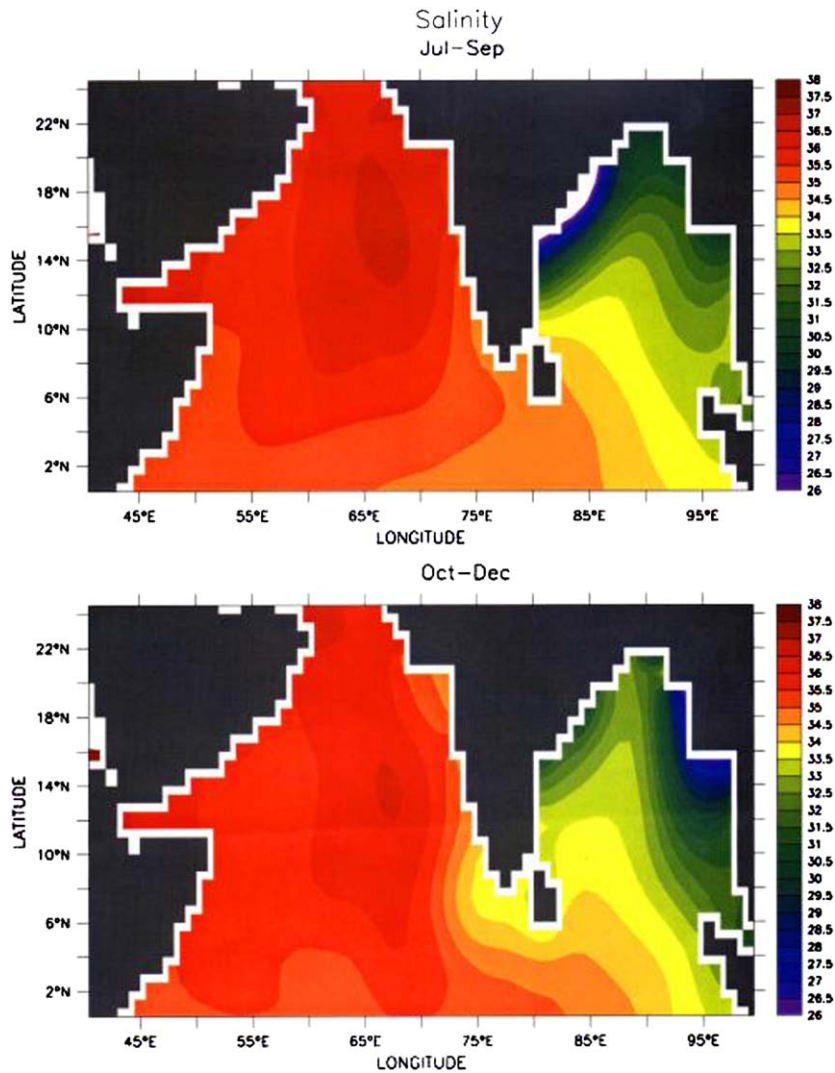


Fig. 9. Salinity variations in the northern Indian Ocean during the SW and the NE monsoons.

Acknowledgments

The authors thank the Directors of the National Institute of Oceanography Dona Paula, Goa and the Space Application Center, Ahmedabad for providing necessary facilities and encouragement. Support of the Officers of the Geological Survey of India and crew of the R.V. *Samudra Kaustubh* of ST 133–136 cruises and Dr. M. Bapuji of Regional Research Center Bhubaneswar in collection of water and sediment samples is gratefully acknowledged. JS thanks CSIR for financial support. We

thank Dr. Ali and Professor Nitsuma for constructive and meaningful reviews. This is a contribution of NIO (no. 3989).

References

- Anuradha, T., Suneethi, J., Dash, S.K., Pradhan, Y., Prasad, J.S., Rajawat, A.S., Nayak, S.R., Chauhan, O.S., 2000. Sediment dispersal during NE monsoon over the northern Bay of Bengal: preliminary results using IRS–P4 OCM data. In: Proceedings of the Pacific Ocean Remote Sensing Conference, Goa, India, vol. 2. pp. 813–815.

- Biscaye, P.E., 1965. Mineralogy and sedimentation of recent deep-sea clays in the Atlantic Ocean and adjacent seas and oceans. *Bulletin of Geological Society of America* 76, 803–832.
- Chauhan, O.S., 1995. Monsoon induced temporal changes in the beach morphology and associated sediment dynamics, central east coast of India. *Journal of Coastal Research* 11, 776–787.
- Chauhan, O.S., 2003. Past 20,000-year history of Himalayan Aridity: evidences from oxygen isotope records in the Bay of Bengal. *Current Science* 84, 90–93.
- Chauhan, O.S., Gujar, A.R., 1996. Surficial clay mineral distribution on the southwestern continental margin of India: evidence of input from the Bay of Bengal. *Continental Shelf Research* 16, 321–333.
- Chauhan, P., Nagur, C.R.C., Mohan, M., Nayak, S.R., Navalgund, R.R., 2001. Surface chlorophyll-a distribution in the Arabian Sea and Bay of Bengal using IRS-P4 ocean colour monitor satellite data. *Current Science* 80, 127–129.
- Emmel, F.J., Curray, J.R., 1984. The Bengal submarine fan, Northeastern Indian Ocean. *Geo-Marine Letters* 3, 119–124.
- Emery, W.J., Ikeda, M., 1984. A comparison of geometric correction methods for AVHRR imagery. *Canadian Journal of Remote Sensing* 10, 46–56.
- Ittekkot, V., Nair, R.R., Honjo, S., Ramaswamy, V., Bartsch, M., Mangani, S., Desai, B.N., 1991. Enhanced particle flux in Bay of Bengal induced by injection of fresh water. *Nature* 351, 385–387.
- Konta, J., 1985. In: Degens, T., Kempe, S. (Eds.), *Mineralogy and Chemical Maturity of Suspended Matter in Major Rivers Samples under SCOPE/UNEP, Transport of Carbon and Minerals in Major World Rivers. Part III. Mitteilungen aus dem Geologisch—Paleontologischen Institut der Universität Hamburg*, pp. 569–592.
- Laviolette, P.E., 1967. Temperature, salinity and density of the World's Seas: Bay of Bengal and Andaman Sea. Informal Report No. 67-57 Naval Oceanographic Office, Washington, DC.
- Legeckis, R., Pitchard, J., 1976. Algorithm for correcting the AVHRR imagery for geometric distortions due to the Earth curvature, Earth rotation and spacecraft roll attitude errors. NOAA Technical Memo, NESS 77.
- Levitus, S., Burgett, R., Boyer T.P., 1994. World Ocean Atlas vol. 3, Salinity NOAA Atlas, NESDIS 3, p. 99.
- Mohan, M., Chauhan, P., Mathur, A., Dwivedi, R.M., 1998. Atmospheric correction of MOS-B data using long wavelength and PCI approaches: IRS-P3 MOS validation experiment: Ocean Applications. SAC Report No. SAC/RESA/MWRD/IRSP3/SN/02/98, pp. 14–22.
- Prasad, J.R., Rajawat, A.S., Pradhan, Y., Chauhan, O.S., Nayak, S.R., 2002. Retrieval of sea surface velocities using sequential ocean colour monitor (OCM) data. *Earth Planetary Science* 111, 189–195.
- Rao, V.P., Reddy, N.P.C., Rao, Ch.M., 1988. Clay mineral distribution in the shelf sediments of northern part of the east coast of India. *Continental Shelf Research* 8, 145–151.
- Sarkar, A., Ramesh, R., Bhattacharya, S.K., Rajagopalan, G., 1990. Oxygen isotope evidence for a stronger winter monsoon current during the last glaciation. *Nature* 343, 549–551.
- Shetye, S.R., Shenoi, S.S.C., Gouveia, A.D., Michael, G.S., Sundar, D., Nampoothri, G., 1991. Wind driven coastal upwelling along the western boundary of the Bay of Bengal during southwest monsoon. *Continental Shelf Research* 11, 1397–1408.
- Shetye, S.R., Gouveia, A., Shenoi, S.S.C., Sundar, D., Michael, G.S., Nampoothri, G., 1993. The western boundary current in the seasonal subtropical gyre in the Bay of Bengal. *Journal of Geophysical Research* 98, 945–954.
- Tassan, S., 1994. Local algorithm using SeaWiFS data for retrieval of phytoplankton pigment, suspended sediments and yellow substances in coastal waters. *Applied Optics* 12, 2369–2378.